

Transmission characteristics in plasmonic multimode waveguides

André G. Edelmann · Stefan F. Helfert · Jürgen Jahns

Received: 28 July 2010 / Accepted: 10 January 2011
© Springer Science+Business Media, LLC. 2011

Abstract In this article, we examine spectral transmission characteristics based on the self-imaging effect in plasmonic multimode waveguides. For the analysis, we calculate the correlation between an input field and the field in the self-imaging plane. We perform full vectorial computations using the Method of Lines as numerical method. The resulting transmission profile is discussed with regards to the attenuation, the even and odd mode sets and for several structural parameters of the plasmonic waveguide. The introduced transmission characteristic may offer the opportunity for the implementation of filtering operations in plasmonic waveguides.

Keywords Plasmonic waveguides · Self-imaging effect · Transmission characteristic

1 Introduction

In the domain of plasmonics one deals with electromagnetic waves propagating at optical frequencies along an interface between a dielectric and metallic medium (Raether 1988). The research in that field has received a lot of interest in recent years and is still growing. One aspect of interest refers to plasmonic waveguides, since they may offer opportunities for miniaturization and may even provide a conjunction between optical and electrical circuits (Ozbay 2006; Maier and Atwater 2005).

Plasmonic waves propagating at dielectric-metallic interfaces are called surface plasmon polaritons (SPPs). They can be identified by the property that the maximum of the electromagnetic field is located at the interface and exponentially decays into the dielectric and metallic

A. G. Edelmann (✉) · S. F. Helfert · J. Jahns
FernUniversität in Hagen, Universitätsstr. 27, 58084 Hagen, Germany
e-mail: Andre.Edelmann@FernUni-Hagen.de

S. F. Helfert
e-mail: Stefan.Helfert@FernUni-Hagen.de

J. Jahns
e-mail: Juergen.Jahns@FernUni-Hagen.de

regions. In particular this characteristic is one basic property for miniaturization when dealing with SPPs. In contrast to dielectric waveguides only one interface is necessary to guide electromagnetic waves. From Maxwell's equations we obtain the well-known expression for plasmonic waves $n_{\text{eff}} = \sqrt{\varepsilon_d \varepsilon_m / (\varepsilon_d + \varepsilon_m)}$ (bulk materials). Here the permittivity is given respectively as ε_d and ε_m for the dielectric and metallic material. For plasmon propagation the condition $|\text{Re}(\varepsilon_m)| > \varepsilon_d$ has to be fulfilled. The major challenge in plasmonics results from the high attenuation due to dissipation in the metal. Only short propagation lengths in the range of ten to hundreds of microns can be achieved, depending on the wavelength and the structural parameters of the waveguide. In this context it is important to note that in general plasmonic waveguides with low losses lead to more expansive fields in the adjacent media and vice versa. This dilemma is still an open issue of developments for practical plasmonic waveguides and devices. The plasmonic waveguides considered in this article consist of a small metallic layer surrounded by a dielectric medium (see e.g., Zia et al. 2004; Berini 2000; Edelmann et al. 2010). It is well-known that in such structures two different types of mode sets appear, the even and the odd modes. The even modes have equal signs and the odd modes have opposite signs in the field amplitudes perpendicular to the interface. The nature of surface plasmon polaritons allows two dimensional devices to be developed which can considerably contribute towards miniaturization of electrical and optical circuits. Several devices have previously been developed and analyzed, such as Bragg-gratings and focusing structures (see e.g., Čtyrkyý et al. 1999; Feng et al. 2007).

In this article we suggest transmission profiles in plasmonic multimode waveguides based on the self-imaging effect. The self-imaging phenomenon is examined in dielectric and plasmonic waveguides (see e.g., Soldano and Pennings 1995; Edelmann et al. 2010). Related to this effect we want to find out possibilities for plasmonic devices, in particular for filter applications. For this purpose we use the correlation between the field at the input and at a well-defined position along the plasmonic waveguide. The correlation is useful to quantify the field distribution in the waveguide. The transmission profile is then obtained by the spectral presentation of the correlation coefficient.

We have organized this article as follows: In Sect. 2 we describe the examined plasmonic waveguide and the numerical algorithm we have used; In Sect. 3 the theory of the transmission characteristic is presented. Here we show how the self-imaging effect can be expressed through the correlation coefficient and how it can be used to describe the transmission characteristic; In Sect. 4 we discuss several transmission profiles to quantify, the influence of the attenuation, the even and odd modes and structural parameters. In Sect. 5 we close this article with a conclusion.

2 Examined structure and modelling

In our analysis we use plasmonic waveguides with a rectangular silver metallic layer and surrounded by dielectric media. The cross-section is shown in Fig. 1a. The default values of the structural parameters are: metallic layer thickness $t_m = 0.12 \mu\text{m}$; metallic layer width $w_m = 2.0 \mu\text{m}$; permittivity of the surrounded medium $\varepsilon_d = 4.0$ and the frequency dependent permittivity of silver ε_m is obtained with the Drude model: $\varepsilon_m = \varepsilon_\infty - \omega_p^2 / (\omega^2 - j\gamma\omega)$. Here we use the following parameters taken from (Besbes et al. 2007): $\varepsilon_\infty = 3.36174$, $\omega_p = 1.3388 \times 10^{16} \text{s}^{-1}$, and $\gamma = 7.07592 \times 10^{13} \text{s}^{-1}$. By applying these parameters to the Drude model we obtain $\varepsilon_m = -14.79 - j0.41$ for the wavelength $\lambda_0 = 0.6 \mu\text{m}$ and $\varepsilon_m = -21.34 - j0.65$ for the wavelength $\lambda_0 = 0.7 \mu\text{m}$. In Fig. 1b we have plotted the respective real and

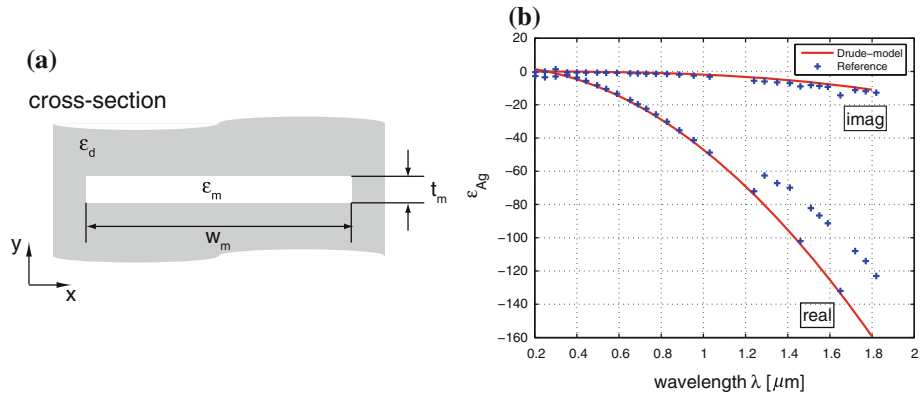


Fig. 1 **a** Cross-section of the plasmonic waveguide. **b** Permittivity ϵ_{Ag} as function of the wavelength: Drude-model (solid curve) and reference values from (Palik 1985) (+)

imaginary part of the permittivity of silver as function of the wavelength together with the reference values taken from (Palik 1985).

In this article we present numerical results gained with full vectorial calculations using the Method of Lines (MoL) (Pregla and Pascher 1989; Pregla 2008). By applying the MoL the cross-section of the plasmonic waveguide is discretized with finite differences (FD). The related wave equation is thereby reduced to $n - 1$ dimensions ($n = 2$ or 3). We obtain the eigenvalues and eigenmodes of the waveguide by combining the FD expressions in an operator matrix and applying a diagonalization step. The MoL has been proven to be a very useful tool for computing the properties of waveguides in microwaves and optics including plasmonics. Since the MoL has been described exhaustively in literature (e.g. Pregla 2008), we will not go into a detailed discussion of it here.

In the calculations that are performed here, we use the discretization values $h_x = 0.05 \mu\text{m}$ and $h_y = 0.02 \mu\text{m}$ in x - and y -direction. This results in 84×76 discretization points in the computation window. In the z -direction the waveguide is homogeneous. This direction describes the direction of wave propagation, which is calculated analytically (by using the MoL). In Fig. 2 we have plotted the first and the third eigenmode of the respective plasmonic waveguide structure shown in Fig. 1a. The shown field distributions refer to the absolute value of the H_x -component ($\lambda_0 = 0.7 \mu\text{m}$, odd modes). It also shows the multimode character of the plasmonic waveguide in x -direction. Further one can see that the maximum of the field amplitude is located at the interfaces in y -direction while it exponentially decays into the dielectric and the metallic region. Note that in the following field distribution images, we always show the field on the upper interface (see Fig. 1a).

Figure 3 shows field distributions of the even-modes and the odd-modes. Here we want to give a more detailed clarification of the notations for these two mode sets. Figure 3a shows the field amplitude of the first eigenmodes in y -direction. The maximum is in both cases located at the interfaces, but for the even-modes we find equal signs in the amplitude and for the odd-modes opposite signs. This situation is similar if we consider the field in x -direction. In Fig. 3b we have plotted the fields of the third eigenmode on the upper and lower interface. On the upper interface we find no difference between the even- and odd-modes. The difference between the mode-sets becomes clear when comparing the fields on the lower interface. Here the even-modes are characterized by equal signs in the field amplitude between the upper and lower interface and the odd-modes with opposite signs.

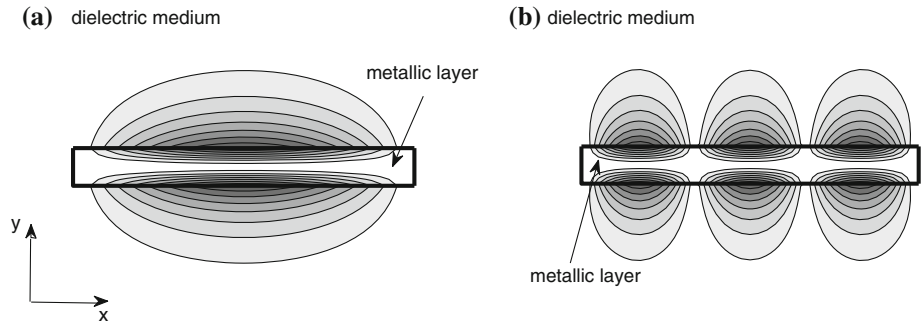


Fig. 2 Field distribution of the absolute value of the H_x -component of the **a** first and **b** third fundamental odd mode. The structure refers to Fig. 1a, the wavelength is chosen with $\lambda_0 = 0.7 \mu\text{m}$ (odd-modes)

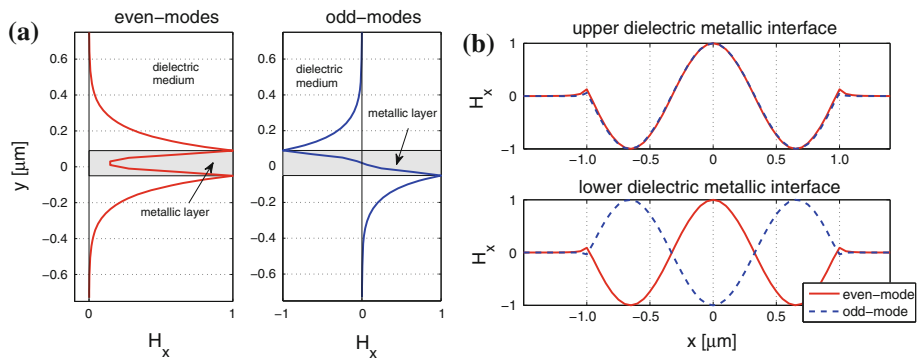


Fig. 3 Field distribution for the even and odd modes in **a** vertical direction for the first eigenmodes and **b** in horizontal direction for the third eigenmodes

3 Theory of the transmission characteristic

The transmission characteristic presented here relates to the previously mentioned self-imaging effect that is well-known in dielectric and in plasmonic multimode waveguides (see e.g., Soldano and Pennings 1995; Edelmann et al. 2010). The self-imaging effect leads to a repetition of an injected field profile at periodic intervals along the direction of wave propagation. In plasmonic waveguides it is important to note that due to the significant attenuation only few self-imaging periods are utilizable, depending on the used wavelength and the structural parameters of the waveguide. Self-imaging occurs due to superposition of the propagated waves within in the waveguide (therefore this effect can only be observed in multimode waveguides) (Soldano and Pennings 1995).

In Fig. 4a we have plotted a two-dimensional plasmonic waveguide structure with metal in the center (ϵ_m) and surrounding dielectric media (ϵ_d). As indicated in Fig. 4a, we inject a narrow field profile in the center of the waveguide. The injected field results from a connected plasmonic waveguide with metallic layer width $w_m = 0.8 \mu\text{m}$. The wave propagates in z -direction and the excitation profile repeats itself in the self-imaging planes. Doubled images can be observed at the center between two primary selfimaging. The length of the period is called L_{si} and means the shortest distance at which self-imaging can occur

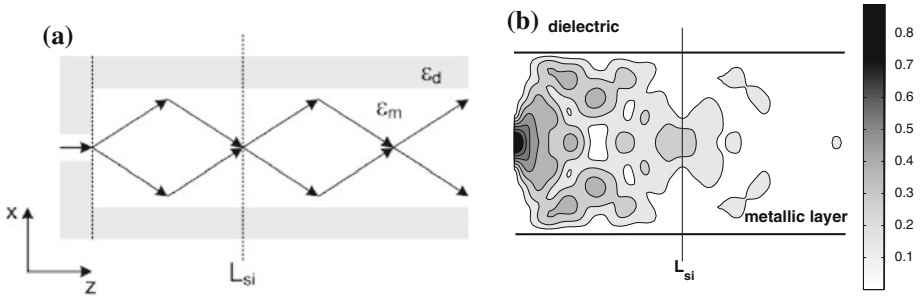


Fig. 4 **a** Principle of the self-imaging effect in multimode waveguides. The input field profile repeats itself at periodic intervals along the direction of propagation (z -direction). **b** Computed field distribution

(Edelmann et al. 2010). For the special case with symmetrical excitation L_{si} can be calculated as follows:

$$L_{si} = \frac{3}{8} \frac{\lambda_0}{\Delta\bar{\beta}}. \tag{1}$$

Here $\Delta\bar{\beta}$ means the propagation constant spacing between the first two fundamental modes of the waveguide (note: $\Delta\bar{\beta}$ is normalized with $k_0 = 2\pi/\lambda_0$). The propagation constant β of the modes depends mainly on the structural parameters: metallic layer thickness t_m , metallic layer width w_m and the dielectric medium ϵ_d of the cladding (see Fig. 1a). Figure 4b shows the computed field distribution (using the MoL) of the $|H_x|$ -component at the wavelength $\lambda_0 = 0.7 \mu\text{m}$ with odd mode excitation. Here we find the injected field profile in the self-imaging plane at the distance L_{si} . It is important to note the decay of the field along the waveguide. The original field amplitude drops to approximately 30% at the first self-imaging plane.

The self-imaging effect can be used to evaluate the suggested transmission characteristic for two reasons. Firstly, self-imaging effect is wavelength-dependent and therefore spectral analysis is made possible. Secondly, if we inject a narrow field profile into the waveguide we obtain the same narrow field profile in the self-imaging plane. In contrast, between these self-images the field is broadened. In the self-imaging plane we can therefore easily couple most of the field into smaller waveguide structures. In Fig. 5 we illustrate these two properties of the self-imaging effect. Figure 5a shows the field distribution determined for the wavelength $\lambda_0 = 0.6 \mu\text{m}$ and Fig. 5b for the wavelength $\lambda_0 = 0.7 \mu\text{m}$ (losses are neglected). For $\lambda_0 = 0.6 \mu\text{m}$ we obtain a self-imaging distance of $L_{si} = 14.8 \mu\text{m}$ and for $\lambda_0 = 0.7 \mu\text{m}$ we obtain $L_{si} = 12.3 \mu\text{m}$. Higher wavelength leads to a shorter self-imaging distances. If we hold the position of the self-imaging plane for the wavelength $\lambda_0 = 0.6 \mu\text{m}$ ($z = 14.8 \mu\text{m}$), see Fig. 5a, and increase the wavelength to $\lambda_0 = 0.7 \mu\text{m}$, see Fig. 5b. We find a significant field broadening at the held position of $z = 14.8 \mu\text{m}$. Assuming that we couple the field at the position of $z = 14.8 \mu\text{m}$ into a smaller waveguide better coupling behavior is achieved for $\lambda_0 = 0.6 \mu\text{m}$ than for $\lambda_0 = 0.7 \mu\text{m}$.

In order to evaluate the transmission behavior we need an adequate quantification of the self-imaging effect in the plasmonic waveguide. Hence we calculate the correlation coefficient between the input field and the field in the self-imaging plane, using Eq. 2.

$$c(z) = \frac{\left| \int H_x(0) \cdot H_x^*(z) dA \right|}{\left| \int H_x(0) dA \right| \cdot \left| \int H_x(z) dA \right|} \tag{2}$$

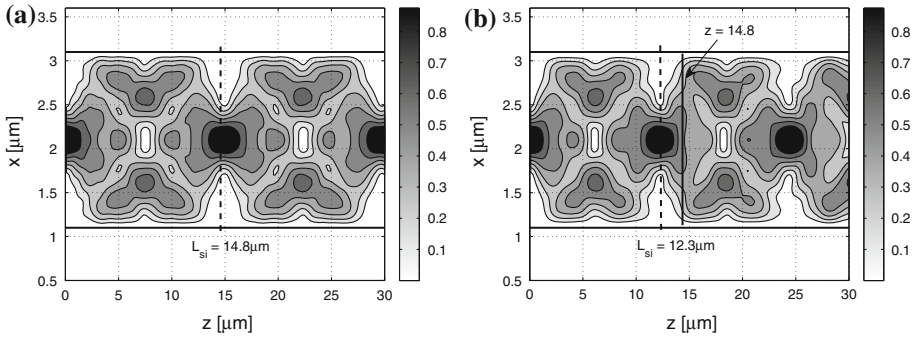


Fig. 5 Field distribution of the absolute value of the H_x -component at the upper dielectric/metallic interface of the plasmonic waveguide for the wavelength **a** $\lambda_0 = 0.6 \mu\text{m}$ and **b** $\lambda_0 = 0.7 \mu\text{m}$ (odd-modes, losses are neglected)

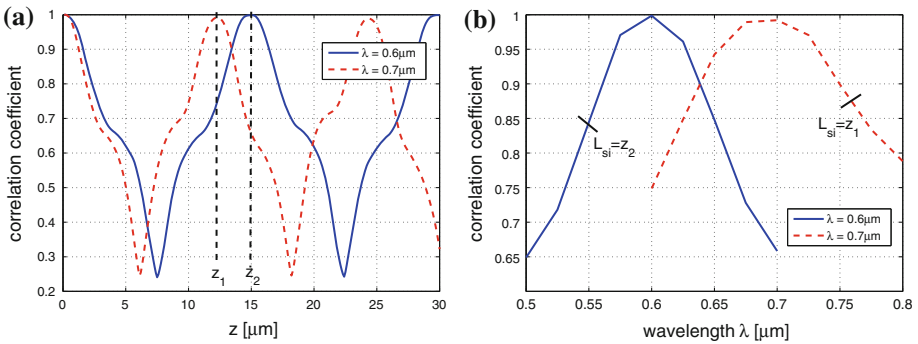


Fig. 6 **a** Correlation coefficient as function of the z direction (direction of wave propagation). **b** Transmission profile (center wavelengths: $\lambda_0 = 0.6 \mu\text{m}$ and $\lambda_0 = 0.7 \mu\text{m}$)

(The integration occurs over the cross-section.) The correlation coefficient allows us to quantify the field broadening as well as the narrow field spot in the self-imaging plane. We have plotted the correlation coefficient related to Fig. 5, in Fig. 6a. Here one can find the correlation coefficient as function of the z -direction (direction of wave propagation) for the wavelength $\lambda_0 = 0.6 \mu\text{m}$ and $\lambda_0 = 0.7 \mu\text{m}$. In the self-imaging plane the correlation coefficient c is close to one. For the self-imaging distances we obtain the maximum correlation for $\lambda_0 = 0.6 \mu\text{m}$ of the value $z_2 = 15.0 \mu\text{m}$ and for $\lambda_0 = 0.7 \mu\text{m}$ of the value $z_1 = 12.3 \mu\text{m}$, which are in good agreement to the self-imaging distances shown in Fig. 5. The value for the correlation coefficient at the position z_2 for $\lambda_0 = 0.7 \mu\text{m}$ is computed with ca. $c_{\lambda=0.7 \mu\text{m}}(z_2) = 0.66$. The respective field broadening can be found in Fig. 5b. The transmission profile is obtained by fixing the position of the first self-imaging plane (e.g. z_2 for the center wavelength $\lambda_0 = 0.6 \mu\text{m}$) and plotting the correlation coefficient as function of the wavelength. The respective transmission profiles are shown in Fig. 6b. We can clearly identify the center wavelength $\lambda_0 = 0.6 \mu\text{m}$ and $\lambda_0 = 0.7 \mu\text{m}$ where the correlation coefficient is close to one. We found decreasing values for correlation the further away the wavelength is from the respective center wavelength. It should be noted that the shape of the transmission profiles also depends on the structural parameters of the plasmonic waveguide.

Fig. 7 Transmission profile for even and odd modes (wavelength: $\lambda_0 = 0.6 \mu\text{m}$, losses are neglected)

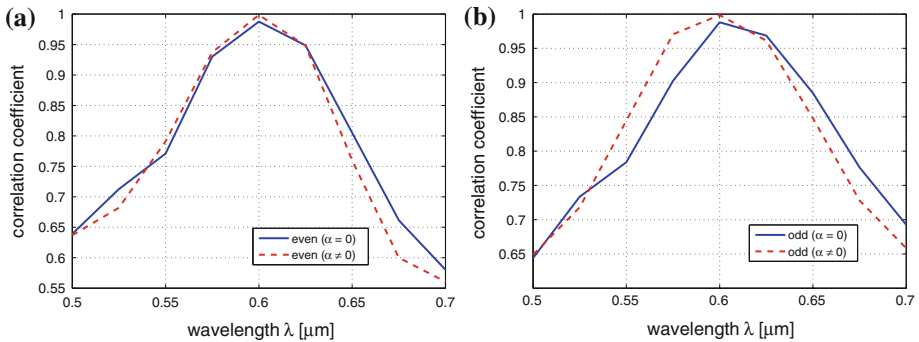
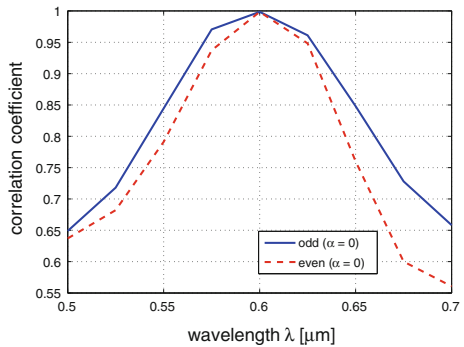


Fig. 8 Transmission profile for **a** even and **b** odd modes with attenuation neglected and taken into account (wavelength $\lambda_0 = 0.6 \mu\text{m}$)

4 Numerical results

In this section, we will show transmission profiles and discuss the difference between even and odd modes, the influence of the attenuation and structural parameters of the plasmonic waveguide. Further we place an output waveguide at the self-imaging distance, measure the output power and compare the values with the correlation coefficient. The results shown here refer to the plasmonic waveguide structure shown in Fig. 1a using the default values described in Sect. 2 unless stated otherwise. At first we analyze the difference between even and odd modes using the center wavelength $\lambda_0 = 0.6 \mu\text{m}$, see Fig. 7. Here we have neglected the attenuation of the waveguide. As shown, the curve for the odd modes is above the curve of the even modes. This means that the even modes are slightly more wavelength selective and their field is broadened faster in the self-imaging plane. In Fig. 8 we take the attenuation into account. One can find similar profiles for the even and odd modes. This means that in both cases the curves with neglected attenuation are below the curves with attenuation taken into account below the center wavelength. Above the center wavelength the profiles cross and the curve with neglected attenuation is above the other. This results from the wavelength dependent nature of the attenuation constant. For higher wavelengths the attenuation constant decreases and the propagation constant spacing $\Delta\beta$ (see Eq. 1) increases and leads to the effect in Fig. 8. Additionally, the drop of the field amplitude because of the attenuation does not affect the transmission profile.

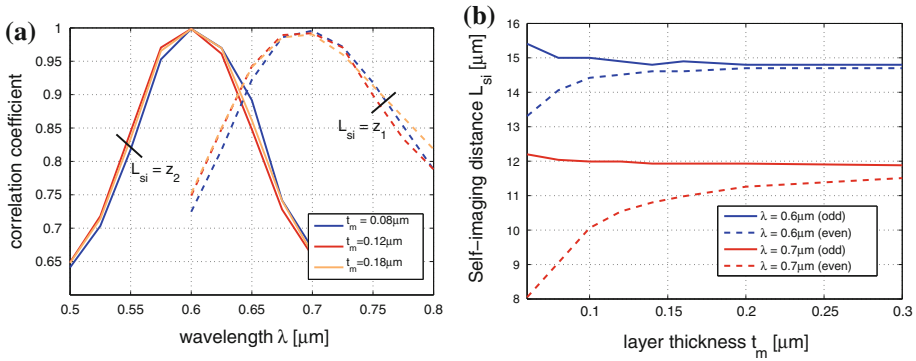


Fig. 9 **a** Transmission profile for different values of the layer thickness t_m and **b** dependency of the self-imaging distance L_{si} on the layer thickness t_m (wavelengths: $\lambda_0 = 0.6 \mu\text{m}$ and $\lambda_0 = 0.7 \mu\text{m}$, odd modes, losses are neglected)

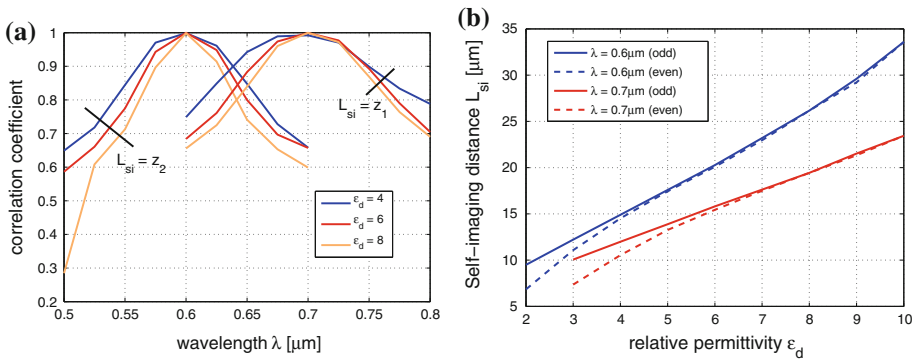


Fig. 10 **a** Transmission profile for different values of the surrounded dielectric medium ϵ_d and **b** dependency of the self-imaging distance L_{si} on the surrounded dielectric medium ϵ_d (wavelengths: $\lambda_0 = 0.6 \mu\text{m}$ and $\lambda_0 = 0.7 \mu\text{m}$, odd modes, losses are neglected)

Next we discuss the influence of the metallic layer thickness t_m and the surrounding dielectric medium ϵ_d regarding the transmission profile. In Fig. 9a we consider two transmission profiles for the center wavelengths of $\lambda_0 = 0.6 \mu\text{m}$ and $\lambda_0 = 0.7 \mu\text{m}$ and vary the values for the metallic layer thickness t_m . For both center wavelengths, no significant changes can be observed. This behavior can be explained by Fig. 9b. Here we have plotted the self-imaging distance L_{si} of the even and odd modes as function of the layer thickness t_m . These curves were calculated with Eq. 1, the contained value for the propagation constant spacing $\Delta\beta$ was obtained from numerical calculations.

As shown in Fig. 9b, the odd-modes are nearly unaffected by the value for t_m whereas the even modes show an increasing difference for small values of t_m . This is in good agreement with the observed transmission profiles, since the odd-modes are used. Again in Fig. 10a we consider the center wavelengths $\lambda_0 = 0.6 \mu\text{m}$ and $\lambda_0 = 0.7 \mu\text{m}$, but here we vary the values of the surrounded dielectric medium ϵ_d . In this case we found significant deviation in the transmission profile. Results showing strong dependency of the self-imaging distance L_{si} on the value ϵ_d , can be seen in Fig. 10b. The finding presented in Figs. 9 and 10, were calculated by neglecting the attenuation of the plasmonic waveguide.

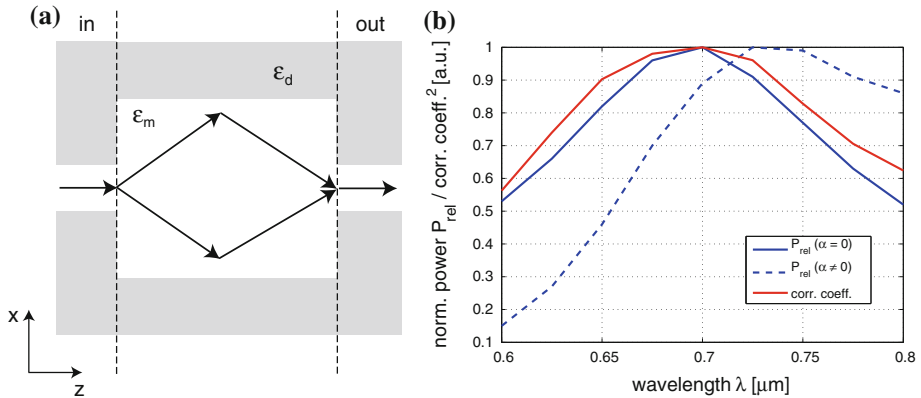


Fig. 11 **a** Filtering structure: an output waveguide is placed in the first self-imaging plane of the plasmonic waveguide. **b** Transmission profile for the transmitted normalized power ($P_{\max} = 0.91$ for neglected attenuation and $P_{\max} = 0.18$ for considered attenuation) and the square correlation coefficient (wavelength $\lambda_0 = 0.7 \mu\text{m}$)

Now we place an output waveguide (with the same dimension as the input waveguide) in the first self-imaging plane of the plasmonic waveguide, see Fig. 11a. We calculate the transmitted power of the first fundamental odd-mode of the input waveguide (with neglected and considered attenuation). In Fig. 11b we have compared these results with the correlation coefficient shown in Fig. 6b. Since the correlation coefficient relates to the field we use its square to compare it with the power. The transmitted power is normalized to the maximal power ($P_{\max} = 0.91$ for neglected attenuation and $P_{\max} = 0.18$ for considered attenuation). The curves refer to the center wavelength $\lambda_0 = 0.7 \mu\text{m}$. One can see in Fig. 11b that in case of neglected attenuation the curves of the square correlation coefficient and the transmitted power are close to each other. The transmitted power is slightly below the square correlation coefficient. Here we have to note that in case of the correlation coefficient no reflections occur because this values refer to the structure in Fig. 4a. If we take the attenuation into account, we found significant deviation in comparison to the other curves. We find a shift of the maximum power to higher wavelength and an asymmetric spectral characteristic. This results from the decreasing attenuation by an increase of wavelength.

5 Conclusion

In this article we have examined transmission characteristics based on the self-imaging effect in plasmonic multimode waveguides. For this purpose we determined the correlation coefficient between the injected field and the field in the self-imaging plane (for the chosen wavelength). We kept the wavelength-dependent self-imaging distance L_{si} constant and varied the wavelength. We obtained the transmission profiles by plotting the correlation coefficient as function of the wavelength. We have discussed the transmission profile in reference to the difference between the even and odd modes, the attenuation, the metallic layer thickness t_m and the surrounded dielectric media ϵ_d . The dependency of several parameters (e.g., ϵ_d) regarding the transmission profile could be interesting for the analysis of plasmonic waveguides. Additionally we have compared the results for the correlation coefficient with the transmitted power in a filtering structure. If we neglect the attenuation we found a good agreement of

the curves. If we consider the attenuation the transmission profiles differ significant from the other curves. This is an interesting issue for further inspections. The presented transmission characteristics follow from the broadening of the field in the plasmonic waveguide. Filtering effects may be achieved by specific output waveguides that are positioned in the self-imaging plane with e.g. smaller layer width or specific structuring (Helfert et al. 2009).

Acknowledgments We thank Christopher Alain Jones for reading this manuscript.

References

- Berini, P.: Plasmon-polariton waves guided by thin lossy metal films of finite width: bound modes of symmetric structures. *Phys. Rev. B* **61**(15), 10484–10503 (2000)
- Besbes, M., Hugonin, J., Lalanne, P., van Haver, S., Janssen, O., Nugrowati, A., Xu, M., Pereira, S., Urbach, H., van de Nes, A., Bienstman, P., Granet, G., Moreau, A., Helfert, S., Sukharev, M., Seideman, T., Baida, F., Guizal, B., Labeke, D.V.: Numerical analysis of a slit-groove diffraction problem. *J. Eur. Opt. Soc.* **2**, 07022 (2007)
- Čtyroký, J., Abdelmalek, F., Ecke, W., Usbeck, K.: Modelling of the surface plasmon resonance waveguide sensor with bragg grating. *Opt. Quant. Electron.* **31**, 927–941 (1999)
- Edelmann, A.G., Helfert, S.F., Jahns, J.: Analysis of the self-imaging effect in plasmonic multimode waveguides. *Appl. Opt.* **49**(7), A1–A10 (2010)
- Feng, L., Tetz, K., Slutsky, B., Lomakin, V., Fainman, Y.: Fourier plasmonics: diffractive focusing of in-plane surface plasmon polariton waves. *Appl. Phys. Lett.* **91**, 081101 (2007)
- Helfert, S., Huneke, B., Jahns, J.: Self-imaging effect in multimode waveguides with longitudinal periodicity. *J. Eur. Opt. Soc.* **4**, 09031 (2009)
- Maier, S.A., Atwater, H.A.: Plasmonics: Localization and guiding of electromagnetic energy in metal/dielectric structures. *J. Appl. Phys.* **98**, 011101 (2005)
- Ozby, E.: Plasmonics: merging photonics and electronics at nanoscale dimensions. *Science* **311**, 189–193 (2006)
- Palik, E.D.: *Handbook of Optical Constants of Solids*. Academic Press, London (1985)
- Pregla, R.: *Analysis of electromagnetic Fields and Waves: The Method of Lines*. Wiley, West Sussex (2008)
- Pregla, R., Pascher, W.: The method of lines. In: Itoh, T. (ed.) *Numerical Techniques for Microwave and Millimeter Wave Passive Structures*, pp. 381–446. Wiley, New York (1989)
- Raether, H.: *Surface Plasmons on Smooth and Rough Surfaces and on Gratings*. Springer, Berlin (1988)
- Soldano, L.B., Pennings, E.C.M.: Optical multi-mode interference device based on self-imaging: principles and applications. *J. Lightwave Technol.* **13**, 615–627 (1995)
- Zia, R., Selker, M.D., Catrysse, P.B., Brongersma, M.L.: Geometries and materials for subwavelength surface plasmon modes. *J. Opt. Soc. Am. A* **21**(12), 2442–2446 (2004)